Maximum of a Fractional Brownian Motion: Analytic Results from Perturbation Theory

Mathieu Delorme and Kay Jörg Wiese
CNRS-Laboratoire de Physique Théorique de l'Ecole Normale Supérieure, 24 rue Lhomond, 75005 Paris, France
(Received 23 July 2015; published 20 November 2015)

Fractional Brownian motion is a non-Markovian Gaussian process X_t, indexed by the Hurst exponent H. It generalizes standard Brownian motion (corresponding to $H = 1/2$). We study the probability distribution of the maximum m of the process and the time $t_{\max}$ at which the maximum is reached. They are encoded in a path integral, which we evaluate perturbatively around a Brownian, setting $H = 1/2 + \varepsilon$. This allows us to derive analytic results beyond the scaling exponents. Extensive numerical simulations for different values of H test these analytical predictions and show excellent agreement, even for large ε.

DOI: 10.1103/PhysRevLett.115.210601 PACS numbers: 05.40.Jc, 02.50.Cw, 87.10.Mn

Random processes are ubiquitous in nature. While averaged quantities have been studied extensively and are well characterized, it is often more important to understand the extremal behavior of these processes [1] associated with failure in fracture or earthquakes, a crash in the stock market, the breakage of dams, etc. Though many processes can be successfully modeled by Markov chains and are well analyzed by the tools of statistical mechanics, there are also interesting and realistic systems which do not evolve with independent increments, and thus are non-Markovian, i.e., history dependent. Dropping the Markov property, but demanding that a continuous process be scale invariant and Gaussian with stationary increments defines an enlarged class of random processes, known as fractional Brownian motion (fBM). Such processes appear in a broad range of contexts: Anomalous diffusion [2], polymer translocation through a pore [3–5], the dynamics of a tagged monomer [6,7], finance (fractional Black-Scholes and fractional stochastic volatility models [8]), hydrology [9], and many more.

FBM is a generalization of standard Brownian motion to other fractal dimensions, introduced in its final form by Mandelbrot and Van Ness [10]. It is a Gaussian process $(X_t)_{t\in\mathbb{R}}$, starting at zero, $X_0 = 0$, with mean $\langle X_t\rangle = 0$ and covariance function (variance)

$$\langle X_t X_s\rangle = s^{2H} + t^{2H} - |t-s|^{2H}. \tag{1}$$

The parameter $H \in (0,1)$ is the Hurst exponent; the process typically grows with time as t^H. Standard Brownian motion corresponds to $H = 1/2$; there the covariance function reduces to $\langle X_t X_s\rangle = 2\min(s,t)$. Unless $H = 1/2$, the process is non-Markovian, i.e., its increments are not independent: For $H > 1/2$ they are correlated, whereas for $H < 1/2$ they are anticorrelated,

$$\langle \partial_t X_t \partial_s X_s\rangle = 2H(2H-1)|s-t|^{2(H-1)}. \tag{2}$$

In this Letter we study the *maximum* of a fractional Brownian motion $m = \max_{t\in[0,T]} X_t$ and the time $t_{\max}$ when this maximum is reached [11] with the initial condition $X_0 = 0$ and total time $T > 0$. Figure 1 shows an illustration for different values of H, using the same random numbers for the Fourier modes. We will denote $P_H^T(m)$ and $P_H^T(t)$ their respective probability distributions. Previous studies can be found in Refs. [13,14].

These observables are closely linked to other quantities of interest, such as the first-return time, the survival probability, the persistence exponent, and the statistics of records. Though studied for a long time, most results for non-Markovian processes are quite recent [15–17].

Following the ideas of Refs. [18–20], we encode our observables $P_H^T(m)$ and $P_H^T(t)$ in a path integral,

$$Z^+(m_1,t_1;x_0;m_2,t_2) = \int_{X_0=m_1}^{X_{t_1+t_2}=m_2} \mathcal{D}[X]\Theta[X]\delta(X_{t_1}-x_0)e^{-S[X]}. \tag{3}$$

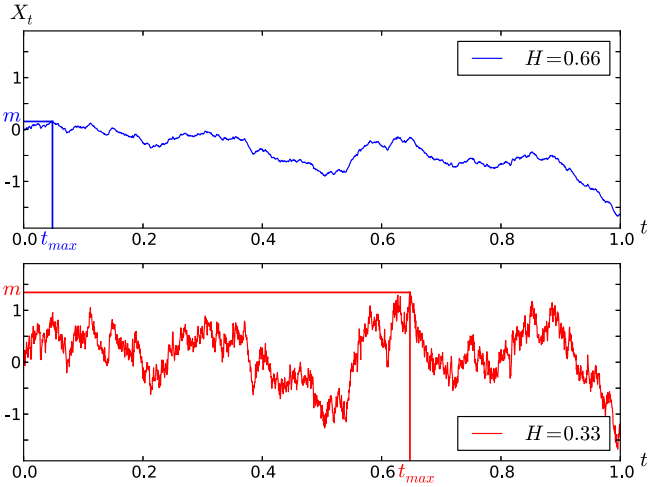

FIG. 1 (color online). Two realizations of fBM paths for different values of H, generated using the same random numbers for the Fourier modes in the Davis and Harte procedure [12]. The observables m and $t_{\max}$ are given.

This sums over all paths X_t, weighted by their probability $e^{-S[X]}$, starting at $X_0 = m_1 > 0$ (shifted for convenience), passing through x_0 (close to 0) at time t_1, and ending in $X_{t_1+t_2} = m_2 > 0$, while staying *positive* for all $t \in [0, t_1 + t_2]$. The latter is enforced by the product of Heaviside functions $\Theta[X] := \prod_{s=0}^{t_1+t_2} \Theta(X_s)$.

As X_t is a Gaussian process, the action S can (at least formally) be constructed from the covariance function of X_t. However, this is not enough to evaluate the path integral (3) in all generality. Following the formalism of Ref. [20], we use standard Brownian motion as a starting point for a perturbative expansion, setting $H = \frac{1}{2} + \varepsilon$ with ε a small parameter; then the action at first order in ε is (we refer to the appendix of Ref. [20] for the derivation)

$$S[X] = \frac{1}{4D_{\varepsilon,\tau}} \int_0^T \dot{X}_{\tau_1}^2 d\tau_1 - \frac{\varepsilon}{2} \int_0^{T-\tau} d\tau_1 \int_{\tau_1+\tau}^T d\tau_2 \frac{\dot{X}_{\tau_1} \dot{X}_{\tau_2}}{|\tau_2 - \tau_1|} + O(\varepsilon^2). \quad (4)$$

The time τ is a regularization cutoff for coinciding times (one can also introduce discrete times spaced by τ [20]). The first line is the action for standard Brownian motion, with a rescaled diffusion constant [21] $D_{\varepsilon,\tau} = 1 + 2\varepsilon[1 + \ln(\tau)] + O(\varepsilon^2) \simeq (e\tau)^{2\varepsilon}$. The second line is a correction, nonlocal in time since fBM is non-Markovian.

Computing the ε expansion of Eq. (3) using Eq. (4) is rather technical. A graphical representation of the key term is given in Fig. 2. The result for $Z^+(m_1, t_1; x_0; m_2, t_2)$ covers a page, presented in Ref. [22]. We use this result here to deduce its most interesting implications, starting with the probability distribution of $t = t_{\max}$. For Browanian motion ($H = 1/2$), this distribution is well known as the Arcsine law [23],

$$P_{1/2}^T(t) = \frac{1}{\pi\sqrt{t(T-t)}}, \quad \text{for } t \in [0, T]. \quad (5)$$

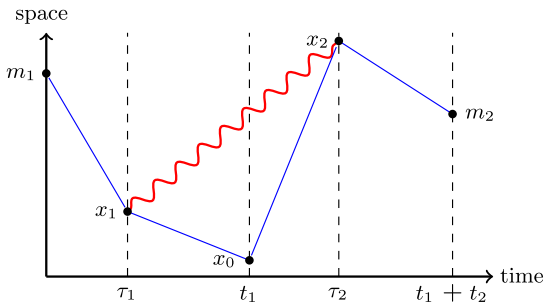

FIG. 2 (color online). Graphical representation of a contribution to the path-integral $Z^+(m_1, t_1; x_0; m_2, t_2)$ given in Eq. (3). The red curve represents the nonlocal interaction in the action [second line of Eq. (4)] while blue lines are bare propagators. There are two other contributions when the time ordering is $\tau_1 < \tau_2 < t_1$ or $t_1 < \tau_1 < \tau_2$, already computed in Ref. [20].

Until now, only scaling properties were known for this distribution in the general case [24]. The path integral (3) is linked to this distribution via

$$P_H^T(t) = \lim_{x_0 \to 0} \frac{1}{Z} \int_{m_1, m_2 > 0} Z^+(m_1, t; x_0; m_2, T - t). \quad (6)$$

The normalization Z depends on x_0 and T. Our result for the distribution of $t_{\max}$ takes a nice form if we exponentiate the order-ε correction obtained from Eq. (6),

$$P_H^T(t) = \frac{1}{[t(T-t)]^H} \exp\left(\varepsilon \mathcal{F}\left(\frac{t}{T-t}\right)\right) + O(\varepsilon^2). \quad (7)$$

This is plotted on Fig. 3. We see the expected change in the scaling form of the Arcsine law, $\sqrt{t(T-t)} \to [t(T-t)]^H$ and a nontrivial change in the shape given by the function

$$\mathcal{F}(u) = \sqrt{u}[\pi - 2\arctan(\sqrt{u})] + \frac{1}{\sqrt{u}}\left[\pi - 2\arctan\left(\frac{1}{\sqrt{u}}\right)\right] + \text{cst}. \quad (8)$$

The time reversal symmetry $t \to T - t$ (corresponding to $u \to u^{-1}$) is explicit; the constant ensures normalization.

We tested the prediction (7)–(8) with numerical simulations of a discretized fractional Brownian motion for different values of H. To this aim, we used the Davis and Harte procedure as described in Ref. [12] (and references therein). To compare numerical results with the theory, we extract an estimation $\mathcal{F}_{\text{num}}^{\varepsilon}$ of the function $\mathcal{F}$ as

$$\mathcal{F}_{\text{num}}^{\varepsilon}\left(\frac{t}{T-t}\right) := \frac{1}{\varepsilon} \ln\left(P_{\text{num}}^{T,H}(t)[t(T-t)]^H\right). \quad (9)$$

Here, $P_{\text{num}}^{T,H}(t)$ is the numerical estimation of the distribution of $t_{\max}$ for the discretized fBM at given H (obtained with uniform binning). Apart from discretization effects, we

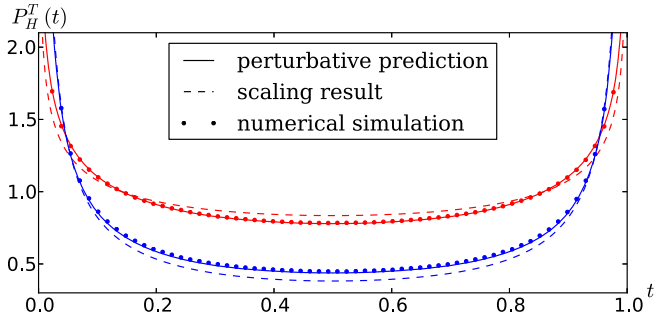

FIG. 3 (color online). Distribution of $t_{\max}$ for $T = 1$ and $H = 0.25$ (red) or $H = 0.75$ (blue) given in Eq. (7) (plain lines) compared to the scaling ansatz, i.e., $\mathcal{F} = \text{cst}$ (dashed lines) and numerical simulations (dots). For $H < 0.5$ realizations with $t_{\max} \approx T/2$ are less probable (by about 10%) than expected from scaling. For $H > 0.5$ the correction has the opposite sign.

should see significant statistical errors as $\varepsilon \to 0$, and systematic order-ε^2 corrections for larger ε. As can be seen on Figs. 3 and 4, our numerical and analytical results are in remarkable agreement for all values of H studied, both for ε *positive* and *negative*. As an example, for $H = 0.75$, the correction to the pure scaling distribution has a relative magnitude of 10% (see Fig. 3), which is measured in our simulation with a relative precision of 0.5%. This precision even allows us to numerically extract the subleading $O(\varepsilon^2)$ correction; see Fig. 4 right.

We now present results for the distribution of the maximum $P_H^T(m)$. For Brownian motion

$$P_{\frac{1}{2}}^T(m) = \frac{e^{-m^2/(4T)}}{\sqrt{\pi T}}, \quad m > 0. \tag{10}$$

On the other hand, not much is known for generic values of H. This distribution is of interest, as it is linked to the survival probability $S(T,x)$, and the persistence exponent θ. The latter is defined for any random process X_t with $X_0 = x$ as

$$S(T,x) = \text{prob}(X_t \geq 0 \quad \text{for all } t \in [0,T]) \underset{T\to\infty}{\sim} T^{-\theta_x}. \tag{11}$$

For a large class of processes the exponent θ is independent of x. For fractional Brownian motion with Hurst exponent H it was shown that $\theta_x = \theta = 1 - H$ [14,25]. To understand the link of $S(T,x)$ with the maximum distribution for fBM, we use self affinity of the process X_t to write $P_H^T(m)$ as

$$P_H^T(m) = \frac{1}{\sqrt{2}T^H} f_H\left(\frac{m}{\sqrt{2}T^H}\right). \tag{12}$$

Here, f is a scaling function depending on H. Equation (10) can be reformulated as $f_{1/2}(y) = \sqrt{2/\pi}e^{-y^2/2}$. The survival probability is related to the maximum distribution by

$$S(T,x) = \int_0^x P_H^T(m)dm = \int_0^{x/(\sqrt{2}T^H)} f_H(y)dy. \tag{13}$$

This states that a realization of a fBM starting at x and remaining positive is the same as a realization starting at 0 with a minimum larger than $-x$, due to translation invariance of the fBM. Finally, the symmetry $x \to -x$ gives the correspondence between minimum and maximum.

These considerations allow us to predict the scaling behavior of $P_H^T(m)$ at small m from the large-T behavior of $S(T,x)$ [14],

$$P_H^T(m) \underset{m\to 0}{\sim} m^{(\theta/H)-1} = m^{(1/H)-2}. \tag{14}$$

Using our path integral, we can go further. The maximum distribution can be extracted from Eq. (3),

$$P_H^T(m) = \lim_{x_0\to 0} \frac{1}{Z} \int_0^T dt \int_{m_2>0} Z^+(m,t;x_0;m_2,T-t). \tag{15}$$

Its ε expansion leads to the scaling form of Eq. (12), with

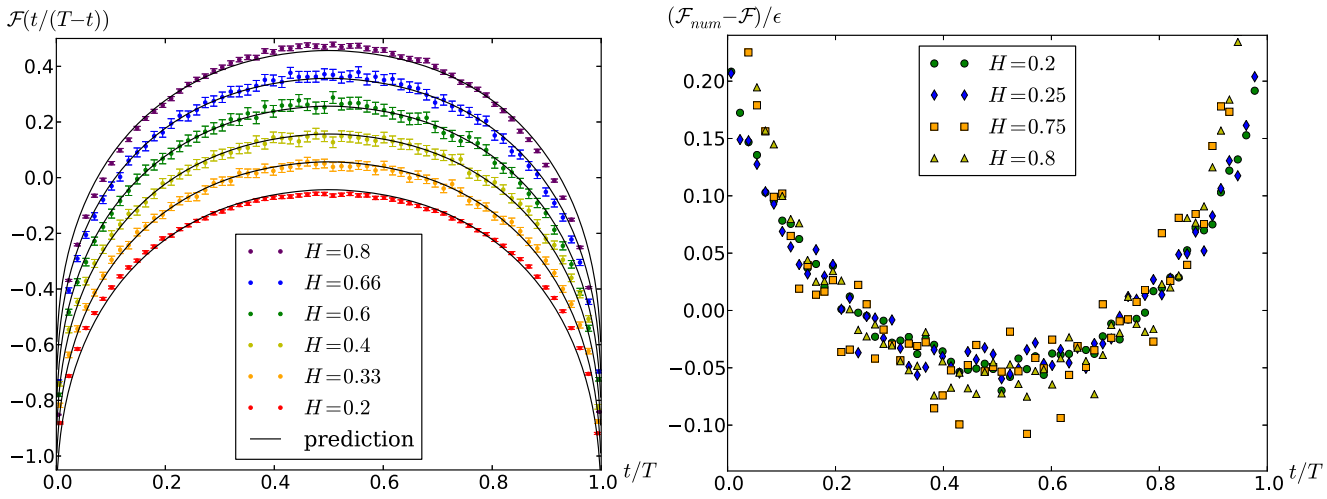

FIG. 4 (color online). Left: Numerical estimation of $\mathcal{F}$ for different values of H on a discrete system of size $N = 2^{12}$, using 10^8 realizations. Plain curves represent the theoretical prediction (8), vertically translated for better visualization. Error bars are 2σ estimates. Note that for $H = 0.6$, $H = 0.66$, and $H = 0.8$ the expansion parameter ε is positive, while for $H = 0.4$, $H = 0.33$, and $H = 0.2$ it is negative. Right: Deviation for large $|\varepsilon|$ between the theoretical prediction (8) and the numerical estimations (9), rescaled by ε. These curves collapse for different values of H, allowing for an estimate of the $O(\varepsilon^2)$ correction to $P_H^T(t)$.

$$f_H(y) = \sqrt{\frac{2}{\pi}} e^{-y^2/2} e^{\varepsilon[\mathcal{G}(y)+\mathrm{cst}]} + O(\varepsilon^2). \quad (16)$$

The constant term ensures normalization. The function $\mathcal{G}$ involves the hypergeometric function ${}_2F_2$:

$$\mathcal{G}(y) = \frac{y^4}{6}\,{}_2F_2\left(1,1;\frac{5}{2},3;\frac{y^2}{2}\right) - 3y^2 + \pi(1-y^2)\mathrm{erfi}\left(\frac{y}{\sqrt{2}}\right) + \sqrt{2\pi}e^{y^2/2}y + (y^2-2)[\gamma_{\mathrm{E}} + \ln(2y^2)]. \quad (17)$$

This function has different asymptotics for small and large y,

$$\mathcal{G}(y) \sim \begin{cases} -2\,\ln(y) & \text{for } y \to \infty \\ -4\,\ln(y) & \text{for } y \to 0 \end{cases}. \quad (18)$$

The second line implies that $P_H^T(m) \sim m^{-4\varepsilon}$ for $m \to 0$, which is consistent (at order ε) with the scaling result (14), $(1/H) - 2 = -4\varepsilon + O(\varepsilon^2)$. Formulas (16)–(17) also predict the distribution at large m. The leading behavior of $P_H^T(m)$ is Gaussian, which is well known, and can be derived from the *Borrel inequality* [26]. Our result for the subleading term can be written as

$$\lim_{y\to\infty} \frac{\ln\left(f_H(y)\exp(\frac{y^2}{2})\right)}{\ln(y)} = -2\varepsilon + O(\varepsilon^2). \quad (19)$$

In order to test these predictions against numerical simulations, we can rewrite the form (16) such that the small-m behavior matches the exact scaling result (14)

$$f_H(y) = \sqrt{\frac{2}{\pi}} e^{-y^2/2} y^{(1/H)-2} e^{\varepsilon[\mathcal{G}(y)+4\ln(y)+\mathrm{cst}]} + O(\varepsilon^2). \quad (20)$$

To extract the nontrivial contribution from numerical simulations, we study for $T = 1$ (see Fig. 5),

$$m^{2-(1/H)} e^{m^2/4} P_{\mathrm{num}}^{1,H}(m) = \exp\left(\varepsilon\left[\mathcal{G}\left(\frac{m}{\sqrt{2}}\right) + 4\ln(m) + \mathrm{cst}\right]\right) + O(\varepsilon^2). \quad (21)$$

The sample size N (i.e., lattice spacing $dt = N^{-1}$) of the discretized fBM used for this numerical test is important, as $P_{\mathrm{num}}(m)$ recovers Brownian behavior for m smaller than a cutoff of order N^{-H}. For small H the necessary system size is very large, so we focus on $H \geq 0.4$. Figure 5 presents results for $H = 0.4$, $H = 0.6$, and $H = 0.75$, without any fitting parameter. The constant term in the scaling form, relevant for normalization, is evaluated numerically. As predicted, convergence to the small-scale behavior is quite slow, especially for $H = 0.4$. This would lead to a wrong numerical estimation of the persistence exponent or other related quantities if the crossover to the large-scale behavior is not properly taken into account. At large scales, the numerical data on Fig. 5 grow as $m^{2\varepsilon}$, consistent with the prediction (19).

To conclude, we have given analytical results for the maximum of a fractional Brownian motion, and the time when this maximum is reached. To our knowledge these are the first analytical results for generic values of H in the range $0 < H < 1$, beyond scaling relations. Comparison to numerical simulations shows excellent agreement, even far from the expansion point $H = \frac{1}{2}$.

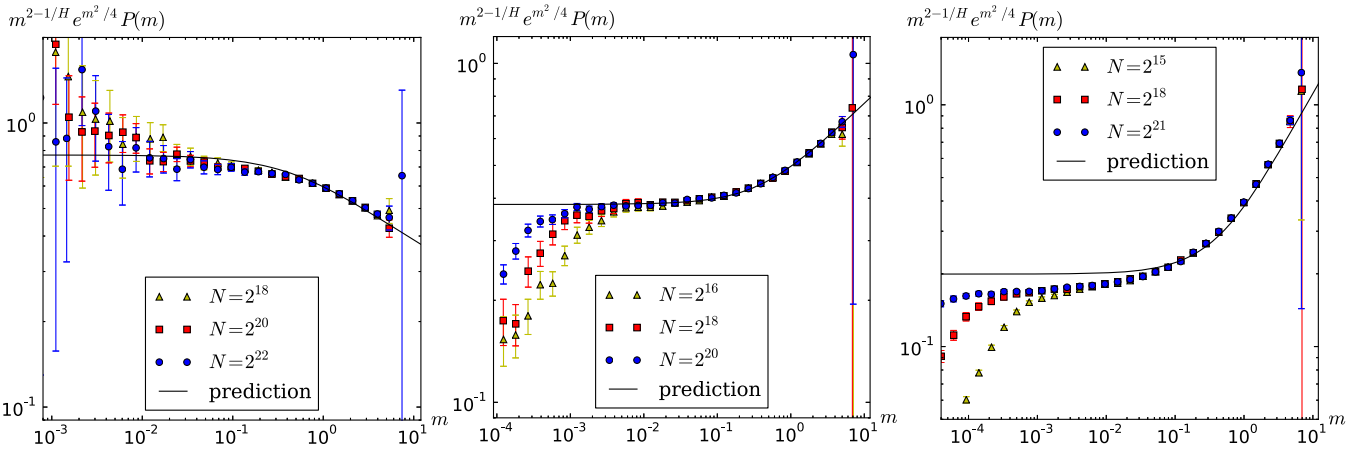

FIG. 5 (color online). The combination (21) for $H = 0.4$ (left), $H = 0.6$ (middle), and $H = 0.75$ (right). The plain lines are the analytical prediction $\exp(\varepsilon[\mathcal{G}(m/\sqrt{2}) + 4\ln(m) + \mathrm{cst}])$ of the maximum without its small-scale power law and large-scale Gaussian behavior. The symbols are numerical estimates for $T = 1$ of the same quantity $m^{2-1/H}\exp(m^2/4)P_{\mathrm{num}}^{T=1,H}(m)$ for different sample sizes. At small scale (of order N^{-H}) discretization errors appear. At large scales the statistics is poor due to the Gaussian prefactor. The large scale behavior on each plot is consistent with the power law $m^{2\varepsilon}$.

Our calculations also gave the joint probability of the maximum, the time when the maximum is reached, and the final point [22]. This allows us to address other observables of interest, such as fractional Brownian bridges.

We thank A. Rosso for stimulating discussions, and PSL for support by Grant No. ANR-10-IDEX-0001-02-PSL.

[1] E. J. Gumbel, *Statistics of Extremes* (Dover, New York, 1958).
[2] J.-P. Bouchaud and A. Georges, Anomalous diffusion in disordered media: statistical mechanisms, models and physical applications, Phys. Rep. **195**, 127 (1990).
[3] A. Zoia, A. Rosso, and S. N. Majumdar, Asymptotic Behavior of Self-Affine Processes in Semi-Infinite Domains, Phys. Rev. Lett. **102**, 120602 (2009).
[4] J. L. A. Dubbeldam, V. G. Rostiashvili, A. Milchev, and T. A. Vilgis, Fractional Brownian motion approach to polymer translocation: The governing equation of motion, Phys. Rev. E **83**, 011802 (2011).
[5] V. Palyulin, T. Ala-Nissila, and R. Metzler, Polymer translocation: the first two decades and the recent diversification, Soft Matter **10**, 9016 (2014).
[6] S. Gupta, A. Rosso, and C. Texier, Dynamics of a tagged monomer: Effects of elastic pinning and harmonic absorption, Phys. Rev. Lett. **111**, 210601 (2013).
[7] D. Panja, Probabilistic phase space trajectory description for anomalous polymer dynamics, J. Phys. Condens. Matter **23**, 105103 (2011).
[8] N. J. Cutland, P. E. Kopp, and W. Willinger, Stock Price Returns and the Joseph Effect: A Fractional Version of the Black-Scholes Model, in *Seminar on Stochastic Analysis, Random Fields and Applications*, edited by E. Bolthausen, M. Dozzi, and F. Russo, Vol. 36 of Progress in Probability (Birkhäuser, Basel, 1995), p. 327.
[9] B. B. Mandelbrot and J. R. Wallis, Noah, Joseph, and operational hydrology, Water Resour. Res. **4**, 909 (1968).
[10] B. B. Mandelbrot and J. W. Van Ness, Fractional Brownian motions, fractional noises and applications, SIAM Rev. **10**, 422 (1968).
[11] These two random variables are almost surely well defined, as realizations of X_t are continuous and realization where the maximum is degenerate are of measure zero.
[12] A. B. Dieker, PhD thesis, University of Twente, 2004.
[13] Y. G. Sinai, Distribution of the maximum of a fractional Brownian motion, Russ. Math. Surv. **52**, 359 (1997).
[14] G. M. Molchan, Maximum of a fractional Brownian motion: Probabilities of small values, Commun. Math. Phys. **205**, 97 (1999).
[15] B. Derrida, V. Hakim, and R. Zeitak, Persistent Spins in the Linear Diffusion Approximation of Phase Ordering and Zeros of Stationary Gaussian Processes, Phys. Rev. Lett. **77**, 2871 (1996).
[16] S. N. Majumdar, Persistence in nonequilibrium systems, Curr. Sci. **77**, 370 (1999).
[17] S. N. Majumdar, A. Rosso, and A. Zoia, Time at which the maximum of a random acceleration process is reached, J. Phys. A **43**, 115001 (2010).
[18] S. N. Majumdar and C. Sire, Survival Probability of a Gaussian Non-Markovian Process: Application to the $T = 0$ Dynamics of the Ising Model, Phys. Rev. Lett. **77**, 1420 (1996).
[19] K. Oerding, S. J. Cornell, and A. J. Bray, Non-markovian persistence and nonequilibrium critical dynamics, Phys. Rev. E **56**, R25 (1997).
[20] K. J. Wiese, S. N. Majumdar, and A. Rosso, Perturbation theory for fractional Brownian motion in presence of absorbing boundaries, Phys. Rev. E **83**, 061141 (2011).
[21] It is a dimensionful constant as fBM and standard Brownian motion do not have the same *time dimension*.
[22] M. Delorme and K. J. Wiese (unpublished).
[23] The cumulative distribution of $t_{\max}$ involves the arcsin function.
[24] S. N. Majumdar, A. Rosso, and A. Zoia, Hitting Probability for Anomalous Diffusion Processes, Phys. Rev. Lett. **104**, 020602 (2010).
[25] F. Aurzada, On the one-sided exit problem for fractional Brownian motion, Electron. Commun. Probab. **16**, 392 (2011).
[26] I. Nourdin, *Selected Aspects of Fractional Brownian Motion*, Bocconi & Springer Series (Springer, New York, 2012).